# Spectroscopic studies of jet-cooled NiAu and PtCu

Eileen M. Spain and Michael D. Morse
*Department of Chemistry, University of Utah, Salt Lake City, Utah 84112*

(Received 16 March 1992; accepted 16 June 1992)

Spectroscopic investigations of NiAu and PtCu have revealed that both molecules possess $^2\Delta_{5/2}$ ground electronic states, and are in this respect analogous to the isovalent molecule NiCu. The ground-state bond lengths ($r_0$) have been measured as $2.351 \pm 0.001$ Å and $2.335 \pm 0.001$ Å for NiAu and PtCu, respectively. Ionization potentials have been bracketed as well, giving IP(NiAu) $= 8.33 \pm 0.38$ eV and IP(PtCu) $= 8.26 \pm 0.07$ eV. A reanalysis of previous high-temperature Knudsen effusion mass spectrometric data provides $D_0^0$(NiAu) $= 2.52 \pm 0.17$ eV. The implications of these results for the electronic structure and chemical bonding of NiAu and PtCu are discussed, and comparison is made to the other diatomic metals of the nickel and copper groups.

## I. INTRODUCTION

In recent years this laboratory has accumulated and interpreted a considerable amount of spectroscopic data for the homonuclear and heteronuclear late transition-metal diatomic molecules. This endeavor has been undertaken in order to identify and examine the important factors that govern the chemical bonding and electronic structure in these species. Previous work includes the study of the heteronuclear copper group diatomics CuAg,[1] CuAu,[2,3] and AgAu,[4] the heteronuclear nickel group diatomics NiPt,[5] PdPt,[6] and NiPd,[6] and a heteronuclear mixed nickel/copper group diatomic, NiCu.[7–9] This work has been supplemented by work on the homonuclear molecules $Cu_2$,[10] $Au_2$,[2,4] $Ni_2$,[11] and $Pt_2$ (Ref. 12) as well. The purpose of these studies has been to use electronic spectroscopy to ascertain the electronic structure of the late transition-metal molecules, thereby obtaining the basic information necessary for understanding the chemical bonding in these species, and in the transition-metal dimers in general. Concepts such as spin–orbit coupling, the presence or absence of *d*-orbital bonding interactions, the relative size of the *s* and *d* orbitals, relativistic effects, and perturbations due to ion-pair states all need to be considered to understand the electronic structure of these species. A review applying these chemical bonding ideas to the late transition-metal diatomics is available[13] and the present investigation of NiAu and PtCu broadens the experimental database for interpretation and verification of these ideas.

In the coinage metal diatomic molecules, two $d^{10}s^1$ atoms combine to form a $^1\Sigma^+_{(g)}$ ground-state molecule. In these systems, *d*-orbital contributions to the chemical bond are essentially absent because the *d* subshells are filled and behave nearly as core orbitals. The chemical bonding in the coinage group diatomics is therefore totally dominated by the *s* orbitals, which overlap to form a two-electron $\sigma$ bond. In the nickel group diatomics, the possibility of *d*-orbital contributions to the chemical bond has been assessed by comparison to the analogous copper group diatomic molecules. In these open *d* subshell molecules, the *d* orbitals are essentially nonbonding in $Ni_2$,[11,13] significant but not overwhelming *d*-orbital bonding is present in NiPd (Refs. 6 and 13) and NiPt,[5,13] and dramatic contributions to the chemical bond are present in $Pt_2$.[12,13] In contrast to these species, which exhibit ground electronic configurations of $d^9_A d^9_B \sigma^2$, diatomic NiCu exhibits a ground configuration of $d^9_{Ni} d^{10}_{Cu} \sigma^2$.[7–9,13,14] The presence of only one *d* hole on the nickel atom makes the electronic structure of this molecule much simpler than that of the $d^9_A d^9_B \sigma^2$ nickel group molecules, and makes it an ideal candidate for detailed study. With this in mind, the electronic structure and chemical bonding of diatomic NiCu have been examined in some detail, both experimentally[7–9] and in one *ab initio* calculation.[14] This has led to important concepts in the chemical bonding of the transition-metal molecules.

The chemical bonding in the ground state of NiCu, deriving from the Ni $3d^9 4s^1(^3D) + $Cu $3d^{10}4s^1(^2S)$ separated atom limit, occurs primarily through the overlap of the atomic *s* orbitals to form a $4s\sigma^2$ molecular orbital. The observation of a $^2\Delta_{5/2}$ ground state[7,8] provides strong evidence that the *d* orbitals remain essentially nonbonding in the $3d^9_{Ni} 3d^{10}_{Cu} \sigma^2$ manifold of states. Nine out of fourteen possible optically allowed transitions from the $X\,^2\Delta_{5/2}$ ground state to the $3d^8_{Ni}(^3F) 3d^{10}_{Cu} \sigma^2 \sigma^{*1}$ excited-state manifold have been observed and identified,[8] allowing the electronic structure of NiCu to be understood in some detail. A simple ligand-field plus spin–orbit theoretical model applied to NiCu has been successful in accounting for the energy-level pattern obtained in *ab initio* calculations on the ground $3d^9_{Ni} 3d^{10}_{Cu} \sigma^2$ manifold of states, and has provided evidence that physical (electrostatic) rather than chemical bonding (overlap) interactions occur between the compact component atom *d* orbitals.[9] The *d*-orbital contribution to the chemical bonding is virtually nil in NiCu, as in $Ni_2$ and $Cu_2$.[13]

Having determined that ligand-field treatments of the $d^9_{Ni} d^{10}_{Cu} \sigma^2$ states of NiCu and the $d^9_A d^9_B \sigma^2$ states of $Ni_2$ are in excellent agreement with *ab initio* results, we have extended our experimental work to systems in which the *d* orbitals are not so compact, NiAu and PtCu. In the former

 0021-9606/92/194605-11$006.00  

molecule, NiAu, the copper ligand of NiCu has been replaced by a gold atom. Although the two atoms are similar in size [$r_e(Cu_2)=2.2197$ Å,[15] $r_e(Au_2)=2.4715$ Å],[16] the $5d$ orbitals of gold are much larger in radial extent than are the $3d$ orbitals of copper [$\langle r_{5d}(Au)\rangle=0.8346$ Å, $\langle r_{3d}(Cu)\rangle=0.5273$ Å].[17] Thus it remains an open question to what extent NiAu may be treated by a ligand–field model, since there is a significant possibility of $d$-orbital overlap, and therefore $d$-orbital bonding in this molecule. In the second molecule, PtCu, the ligand remains a copper atom, but the $d^9$ atom has been changed from nickel to platinum. As in NiAu, this greatly increases the size of the $d$ orbitals, making $d$-orbital contributions to the chemical bonding conceivable [$\langle r_{5d}(Pt)\rangle=0.8746$ Å, $\langle r_{3d}(Ni)\rangle=0.5144$ Å].[17] In addition, however, it greatly increases the spin–orbit splitting of the $d^9$ core ($\zeta_{Ni}=603$ $cm^{-1}$, $\zeta_{Pt}=4052.8$ $cm^{-1}$).[9] Because the density of electronic states is not nearly as severe in NiAu and PtCu as in the corresponding pure nickel group diatomic (NiPt), it is hoped that a study of NiAu and PtCu will shed light on the effects of increased $d$-orbital size and increased spin–orbit splitting on the electronic structure of the late transition-metal molecules.

A concise summary of the methods used to perform these experiments is presented in Sec. II. Low-resolution vibronic spectra for NiAu and PtCu are displayed in Sec. III, along with rotationally resolved spectra for several band systems of the two molecules. In Sec. IV, the results are interpreted and the electronic structure of NiAu and PtCu is discussed and compared to that of NiCu. We conclude our analysis and interpretation in Sec. V with a synopsis of the main points of this work.

## II. EXPERIMENT

Resonant two-photon ionization spectroscopy with time-of-flight mass spectrometric detection has been employed in this investigation, using an apparatus which has been previously described.[18] Diatomic NiAu and PtCu were produced in the throat of a pulsed supersonic nozzle by pulsed laser vaporization of a NiAu (1:1) or PtCu (1:2) alloy target disk. Following expansion into vacuum with helium carrier gas, the beam of jet-cooled diatomic molecules was collimated by a skimmer and admitted into the spectroscopic interrogation and ionization region of a reflectron time-of-flight mass spectrometer. Low-resolution vibronic spectra were collected using a Nd:YAG pumped dye laser to provide the first, exciting photon (YAG denotes yttrium aluminum garnet). The second, ionizing photon was provided by an excimer laser operating on either ArF (193 nm) or $F_2$ (157.6 nm).

For both investigations the alloy target disks were produced by melting the weighed component metals in an electric arc furnace to provide an equimolar alloy of nickel and gold, or in the case of PtCu, a 1:2 molar alloy (Pt:Cu). In the case of PtCu it was decided to employ a 1:2 molar alloy as the laser vaporization target, because the bond strength of $Pt_2$ ($3.14\pm0.02$ eV) (Ref. 12) greatly exceeds that of copper ($2.03\pm0.02$ eV),[13] and probably substantially exceeds that of PtCu as well. In order to limit the destruction of PtCu by the displacement reaction

$$PtCu+Pt\rightarrow Pt_2+Cu, \tag{2.1}$$

it was decided to decrease the amount of platinum in the alloy. In previous studies we have found that this strategy can allow a more weakly bonded heteronuclear molecule [such as CrMo (Ref. 19) or TiV (Ref. 20)] to be produced in significant yield despite the existence of a much more strongly bound homonuclear counterpart [such as $Mo_2$ (Ref. 19) or $V_2$ (Ref. 20)]. Anticipating such difficulties in PtCu, a 1:2 alloy was employed in the first attempt. Although a large concentration of $Pt_2$ was present in the molecular beam, an adequate amount of PtCu was nevertheless produced with the 1:2 PtCu alloy. This approach was not necessary for the production of NiAu because the bond strengths of $Ni_2$ (2.068 eV) (Ref. 11) and $Au_2$ ($2.290\pm0.008$ eV) (Refs. 4 and 21) are not so disparate. In fact, the bond strength of NiAu has been measured by high-temperature mass spectrometry as $2.52\pm0.22$ eV (second-law method) or $2.60\pm0.22$ eV (third law method).[22] Since this exceeds the bond strength of either $Ni_2$ or $Au_2$, it should be a favored product in the cluster source.

Rotationally resolved spectra of both molecules were recorded under high resolution (0.04 $cm^{-1}$) using an intracavity étalon that was inserted into the side-pumped Hänsch configuration dye laser, which was pressure scanned from 0 to 1 atm using Freon-12 ($CCl_2F_2$, DuPont). Absolute frequency calibration was provided by comparison to the well-known absorption spectrum of $I_2$.[23] A final correction was made by taking account of the Doppler shift experienced by the NiAu and PtCu molecules as they traveled toward the light source at the beam velocity of helium, $1.77\times10^5$ cm/s. Ionization potentials were bracketed by recording the optical spectra of NiAu and PtCu twice, once with the energy of the second, ionizing the photon set to 6.42 eV (ArF radiation), and again with it set to 7.87 eV ($F_2$ excimer radiation). Excited-state lifetimes were measured by time-delayed resonant two-photon ionization methods.

## III. RESULTS

### A. Vibronic spectrum of $^{58}Ni^{197}Au$

Figure 1 presents a portion of the vibronic spectrum of the $^{58}Ni$ $^{197}Au$ isotopic modification, collected using coumarin 540A and 500 (Exciton) dye laser radiation for excitation, and ArF excimer radiation (6.42 eV, $\approx$10 mJ/$cm^2$) for photoionization. In the red portion of the spectrum, a single vibrational progression is observed, with an unusually small vibrational frequency of $\omega_e'=79$ $cm^{-1}$, suggesting that the upper state possesses only a shallow potential well. No vibronic hot bands were detected. In addition to this fairly regular vibrational progression, a series of interloper bands are observed, some of which lie very near to the bands forming the progression. Further to the blue a series of intense but very closely spaced transitions are evident near 19 800 $cm^{-1}$. Scans were performed

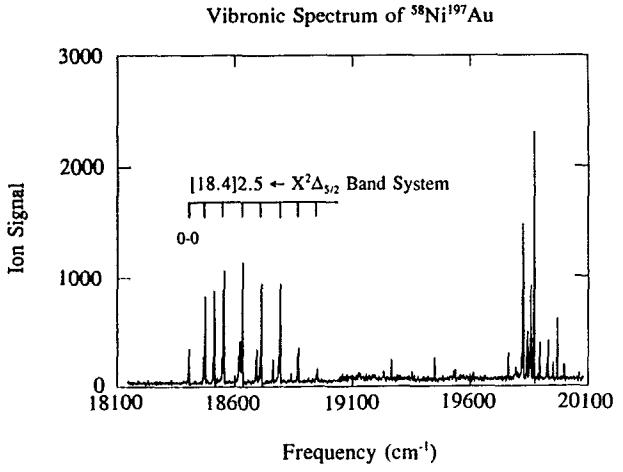


FIG. 1. Low-resolution (0.7 $cm^{-1}$) scan of the vibronic spectrum of $^{58}Ni$ $^{197}Au$, recorded using coumarin 500 and 540 A dye laser radiation in conjunction with ArF radiation for photoionization. The [18.4]2.5$\leftarrow X\,^2\Delta_{5/2}$ vibrational progression is indicated.

further to the blue up to 24 000 $cm^{-1}$, but no spectral features were observed beyond 20 200 $cm^{-1}$. This observation is consistent with rapid predissociation when the energy of the lowest dissociation limit is exceeded, since the bond strength of NiAu measured by high-temperature Knudsen effusion mass spectrometry corresponds to 20 300 ± 1800 $cm^{-1}$ (second-law method) or 21 000 ± 1800 $cm^{-1}$ (third-law method).[22]

Lifetimes measured for the various excited electronic states fall in the range from 6 $\mu$s to 30 $\mu$s. In particular, the 0–0 band of the progression indicated in Fig. 1 displays a lifetime of 6.22 $\mu$s. Assuming that the upper state decays entirely by fluorescence to the ground electronic state, this corresponds to an absorption oscillator strength of $f \approx 7 \times 10^{-4}$, making this band system weakly allowed. The low background signal and high peak intensity is therefore a consequence of a rather large concentration of NiAu molecules in the molecular beam, combined with an inefficient nonresonant two-photon ionization process at the ArF excimer wavelength of 193 nm. Excited-state lifetimes measured for other bands of the observed vibrational progression are listed in Table I. Other measured excited-state lifetimes are listed with the results of rotational analyses in subsequent tables.

## B. Rotationally resolved spectra of $^{58}Ni$ $^{197}Au$

### 1. The 0–0 band of the [18.5]1.5←$X\,^2\Delta_{5/2}$ band system of NiAu

Rather than beginning with the rotational analysis of the bands forming the progression in Fig. 1, it is advantageous to begin the rotational analyses with the "interloper" band at 18 511 $cm^{-1}$, which is displayed in Fig. 2 for the $^{58}Ni$ $^{197}Au$ isotopic modification. This band displays a weak $R$ branch converging toward a bandhead, a stronger $Q$ branch, and a very intense set of $P$-branch lines. The distribution of spectral intensity in the $R$, $Q$, and $P$ branches, with $P > Q > R$, is an immediate indicator of a $\Delta\Omega = -1$ transition according to the Hönl–London intensity formulas.[24] Moreover, it is evident from the large gap between the first lines of the $Q$ and $R$ branches that the ground state possesses a large value of $\Omega''$. A detailed analysis of the spectrum, accompanied by a least-squares fit of the line positions, is in agreement with this conclusion, leading to an assignment of the band shown in Fig. 2 as an $\Omega' = 3/2 \leftarrow \Omega'' = 5/2$ transition. A list of rotational line positions is available[25] from the Physics Auxiliary Publication Service (PAPS) of the American Institute of Physics

TABLE I. The [18.4]2.5$\leftarrow X\,^2\Delta_{5/2}$ system of $^{58}Ni$ $^{197}Au$.

| Band | Measured frequency ($cm^{-1}$) | Fitted frequency ($cm^{-1}$) | Residual ($cm^{-1}$)[a] | Isotope shift ($cm^{-1}$)[b] | Lifetime ($\mu$s) |
|---|---|---|---|---|---|
| 0–0 | 18 402.1483(24)[c,d] | (18 393.378)[e] | (8.77)[d] | −0.86[f] | 6.22 ± 0.29 |
| 1–0 | 18 473.4931(39)[c] | 18 472.832 | 0.660 | −0.11[f] | 6.86 ± 0.09 |
| 2–0 | 18 551.16(5)[c] | 18 552.289 | −1.129 | 0.96[f] | |
| 3–0 | 18 631.4330(45)[c] | 18 631.748 | −0.314 | 2.00[f] | 10.3 ± 1.3 |
| 4–0 | 18 712.06[g] | 18 711.208 | 0.853 | 2.07[g] | |
| 5–0 | 18 791.39[g] | 18 790.671 | 0.720 | 4.14[g] | |
| 6–0 | 18 869.08[g] | 18 870.136 | −1.056 | 3.34[g] | |
| 7–0 | 18 949.87[g] | 18 949.603 | 0.266 | | |

[a]Defined as $\nu - \nu_{calc}$.
[b]Defined as $\nu_0(^{58}Ni\ ^{197}Au) - \nu_0(^{60}Ni\ ^{197}Au)$.
[c]Measured in high resolution (0.04 $cm^{-1}$) as the band origin, $\nu_0$, and calibrated using the $I_2$ atlas. The 1$\sigma$ error limit is given in parentheses.
[d]Not included in the fit.
[e]Bands were fit to the standard expression $\nu = T_0 + \omega_e' v' - \omega_e' x_e' (v'^2 + v')$, resulting in fitted values of $T_0 = 18\,393.38 \pm 1.60\ cm^{-1}$, $\omega_e' = 79.45 \pm 1.03\ cm^{-1}$, and $\omega_e' x_e' = 0.00 \pm 0.11\ cm^{-1}$. This fit was performed omitting the 0–0 band, however, which is experimentally measured to occur 8.77 $cm^{-1}$ to the blue of its predicted position. This shift may imply an unusual shape for the [18.4]2.5 potential curve, or it may result from a homogeneous perturbation which shifts the $v = 0$ level.
[f]Measured in high resolution (0.04 $cm^{-1}$).
[g]Measured in low resolution (0.7 $cm^{-1}$).

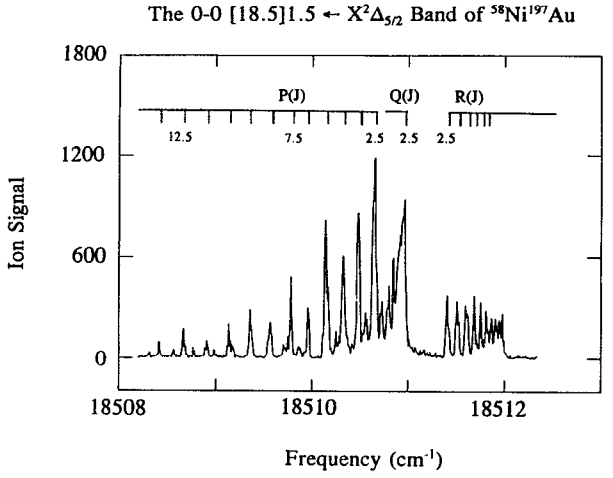


FIG. 2. High-resolution (0.04 $cm^{-1}$) scan over the 0–0 band of the $[18.5]1.5 \leftarrow X\,^2\Delta_{5/2}$ system of $^{58}Ni\ ^{197}Au$. The large gap between the first $Q$ and $R$ lines is indicative of a large value of $\Omega$.

or from one of the authors (M. D. M.). The results of the least-squares fit of the line positions to the standard formula

$$\nu = \nu_0 + B'J'(J'+1) - B''J''(J''+1) \qquad (3.1)$$

are provided in Table II. The observation of an $\Omega''=5/2$ ground state is consistent with the ground state of the congeneric molecule, NiCu,[7,8] and undoubtedly results from the $3d^9_{Ni}5d^{10}_{Au}\sigma^2$ electronic configuration, with the $3d$ hole of the nickel located in the $3d\delta$ orbital. This is also consistent with the predictions of a ligand-field model of the nickel-coinage group mixed diatomics.[9] In addition, since the only $\Omega''=5/2$ Hund's case (a) basis state deriving from the $3d^9_{Ni}5d^{10}_{Au}\sigma^2$ electronic configuration is a $^2\Delta_{5/2}$ state, the ground state of NiAu must remain essentially a pure Hund's case (a) $^2\Delta_{5/2}$ state.

The isotope shift measured for this band $[\nu_0(^{58}Ni\ ^{197}Au) - \nu_0(^{60}Ni\ ^{197}Au) = -1.05\ cm^{-1}]$ is relatively large and negative, and is consistent with a transition in which the vibrational energy content of the upper state is much less than that of the lower state. Given the intensity of the band, it must originate from the $v''=0$ level of the ground electronic state, implying that the vibrational energy content of the upper state is significantly less than the zero-point energy of the ground state. On this basis the band must be assigned as an origin (0–0) band, where the vibrational frequency of the upper state is significantly less than that of the ground state. Although no other bands with $\Omega'=3/2$ have been rotationally resolved, a weak series of bands is observed in the range of 18 600–18 900 $cm^{-1}$, interspersed among the more intense features of the labeled progression. These may well be higher vibrational levels corresponding to the same electronic state as the 0–0 band displayed in Fig. 2. Although these interspersed levels are closely spaced, which is consistent with the low vibrational frequency required for the upper state, they do not follow a very regular pattern and we have not been able to fit them to a simple expression involving $\omega_e$ and $\omega_e x_e$.

In keeping with the notation developed for the rare-earth oxides,[26] the upper state of this band system is identified as the [18.5]1.5 state, where the number in square brackets gives the location of the $v'=0$ level of the upper state in thousands of wave numbers ($cm^{-1}$) above the $v''=0$ level of the ground state, and the $\Omega$ value of this state (1.5) follows the square brackets. This notation has the great advantage that it provides a unique nomenclature for the excited states of a complicated molecule, and should not require relabeling at a later time when more states are discovered and identified.

### 2. The 0–0, 1–0, and 3–0 bands of the $[18.4]2.5 \leftarrow X\,^2\Delta_{5/2}$ band system of NiAu

Having determined that the ground state of NiAu is $^2\Delta_{5/2}$, we may now proceed to a rotational analysis of the bands forming the progression in Fig. 1. Figure 3 presents a rotationally resolved scan over the origin band of this system. Again, this band exhibits a substantial negative isotope shift $[\nu_0(^{58}Ni\ ^{197}Au) - \nu_0(^{60}Ni\ ^{197}Au) = -0.86\ cm^{-1}]$, instead of the more common case of an isotope shift near zero for an origin band. As in the preceding band system, this implies that the zero-point vibrational energy of the ground state substantially exceeds the vibrational energy of the $v'=0$ level of the excited state. This is hardly surprising given the low vibrational frequency of the excited state ($\omega'_e = 79\ cm^{-1}$).

The band displayed in Fig. 3 is representative of the

TABLE II. Results from rotationally resolved studies of $^{58}Ni\ ^{197}Au$.[a]

| System | Band | $\nu_0$ ($cm^{-1}$) | $B'_{v'}$ ($cm^{-1}$) | $B''_0$ ($cm^{-1}$) |
|---|---|---|---|---|
| $[18.5]1.5 \leftarrow X\,^2\Delta_{5/2}$ | 0–0[b] | 18 510.9976(18) | 0.063 90(7) | 0.068 25(7) |
| $[18.4]2.5 \leftarrow X\,^2\Delta_{5/2}$ | 0–0[c] | 18 402.1483(24) | 0.058 77(9) | 0.068 05(8) |
| | 1–0[d] | 18 473.4931(39) | 0.058 28(11) | 0.068 06(11) |
| | 3–0[e] | 18 631.4330(45) | 0.055 86(18) | 0.067 75(19) |
| $\Omega'=5/2 \leftarrow X\,^2\Delta_{5/2}$ | ?–0[f] | 19 867.3737(116) | 0.047 78(40) | 0.067 91(39) |

[a]All values are reported in wave numbers ($cm^{-1}$), with $1\sigma$ error limits in parentheses.
[b]Lifetime of the upper state measured as $\tau = 14.7 \pm 0.5\ \mu s$ ($1\sigma$ error limit).
[c]Lifetime of the upper state measured as $\tau = 6.22 \pm 0.29\ \mu s$ ($1\sigma$ error limit).
[d]Lifetime of the upper state measured as $\tau = 6.86 \pm 0.09\ \mu s$ ($1\sigma$ error limit).
[e]Lifetime of the upper state measured as $\tau = 10.3 \pm 1.3\ \mu s$ ($1\sigma$ error limit).
[f]Lifetime of the upper state measured as $\tau = 6.50 \pm 1.82\ \mu s$ ($1\sigma$ error limit).

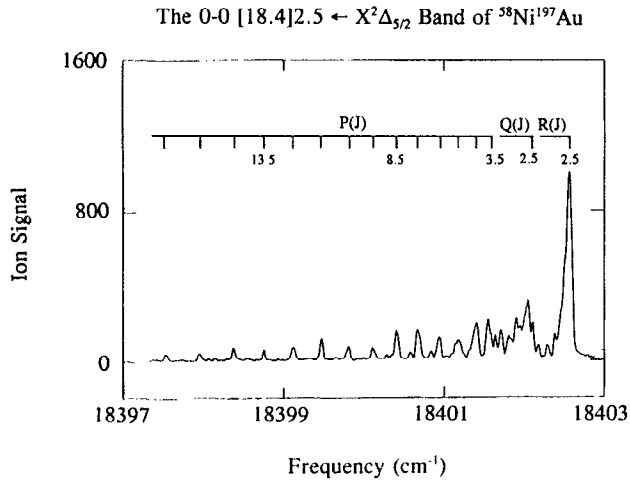


FIG. 3. High-resolution (0.04 $cm^{-1}$) scan over the 0–0 band of the [18.4]2.5$\leftarrow X\,^2\Delta_{5/2}$ system of $^{58}Ni\,^{197}Au$. The spectrum is dominated by an intense bandhead in the $R$ branch, but is nevertheless uniquely assigned as an $\Omega'=5/2\leftarrow\Omega''=5/2$ transition.

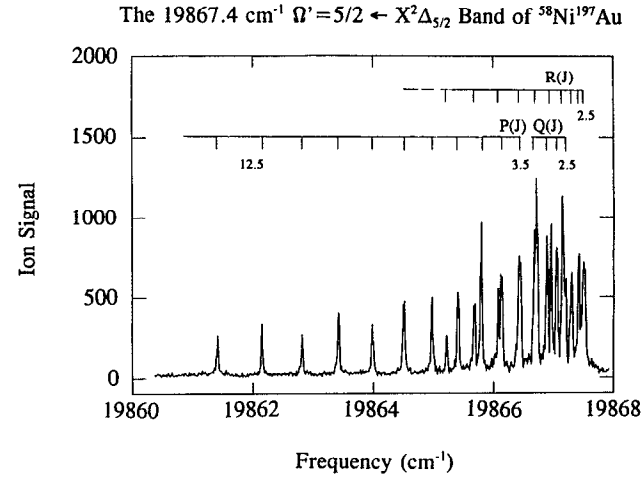


FIG. 4. High-resolution (0.04 $cm^{-1}$) scan over an $\Omega'=5/2\leftarrow X\,^2\Delta_{5/2}$ band of $^{58}Ni\,^{197}Au$. In this case the rotational constants of the upper and lower states are even more disparate than those of Fig. 3, so that returning $R$ lines are well separated and assignable.

0–0, 1–0, and 3–0 bands of the progression labeled in Fig. 1. It is dominated by an intense $R$-branch head, which forms at a low value of $J$. The $Q$ branch is relatively weak and is partially overlapped by returning $R$ lines. The $P$ branch is readily visible out to $J''=16.5$. Spectral simulations using the appropriate Hönl–London factors[24] reproduce the intensity pattern of this band only for a $\Delta\Omega=0$ transition, suggesting an assignment as an $\Omega'=5/2\leftarrow\Omega''=5/2$ band. Detailed analysis of the line positions, accompanied by a least-squares fit, confirms this assignment. A list of rotational line positions and fitted results for this band and all other rotationally resolved bands described in this work is available[25] from the Physics Auxiliary Publication Service (PAPS) of the American Institute of Physics or from one of the authors (M. D. M.). The results of the least-squares fit of the line positions to Eq. (3.1) are provided in Table II for the 0–0, 1–0, and 3–0 bands of the [18.4]2.5$\leftarrow X\,^2\Delta_{5/2}$ system.

### 3. An $\Omega'=2.5\leftarrow X\,^2\Delta_{5/2}$ band of NiAu at 19 867.36 $cm^{-1}$

The most intense band in the NiAu vibronic spectrum shown in Fig. 1 is rotationally resolved and presented in Fig. 4. Based on the observed isotope shift of $\nu_0(^{58}Ni\,^{197}Au)-\nu_0(^{60}Ni\,^{197}Au)=+3.28\ cm^{-1}$ it must be concluded that this is not an origin band. Although the features are well resolved in the spectrum of Fig. 4, it is clear that the band exhibits a very severe head in the $R$ branch, so that returning $R$ lines are interspersed with the other branches. This indicates a large drop in rotational constant, $B$, upon electronic excitation. Assuming that the excited state is relatively free of perturbations, this would correspond to a large increase in bond length upon electronic excitation.

The spectrum of Fig. 4 was analyzed in two steps: first, combination differences were used to assign the lines using the now well-known rotational constant of the ground state, and then a least-squares fit to Eq. (3.1) was employed to extract the rotational constant of the upper state. The observed and fitted line positions are available[25] from the Physics Auxiliary Publication Service (PAPS) of the American Institute of Physics or from one of the authors (M. D. M.). The results of the least-squares fit of the line positions to Eq. (3.1) are provided in Table II. In comparison to the other fitted bands, the quality of the least-squares fit for this band is poor, giving errors of up to 0.06 $cm^{-1}$ in the fitted line positions. The errors in the fitted line positions are similar for the $R(J)$ and $P(J+2)$ lines, however, suggesting a weak perturbation may be present in the upper state. Despite this perturbation, the fitted ground-state rotational constant is in agreement with the previous results.

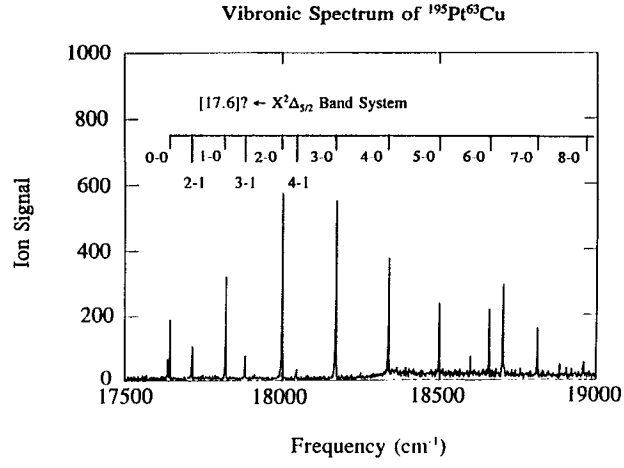


FIG. 5. A portion of the low-resolution (0.7 $cm^{-1}$) spectrum of $^{195}Pt\,^{63}Cu$, recorded using coumarin 540 A, fluorescein 548, and rhodamine 590 dye laser radiation in conjunction with ArF radiation for photoionization. The [17.6]?$\leftarrow X\,^2\Delta_{5/2}$ vibrational progression, which could not be rotationally resolved, is indicated.

TABLE III. The [17.6]?$\leftarrow X\,^2\Delta_{5/2}$ and [19.6]1.5$\leftarrow X\,^2\Delta_{5/2}$ band systems of $^{195}$Pt $^{63}$Cu.

| System | Band | Measured frequency ($cm^{-1}$) | Fitted frequency ($cm^{-1}$)[a] | Residual ($cm^{-1}$)[b] | Isotope shift ($cm^{-1}$)[c] | Lifetime ($\mu s$) |
|---|---|---|---|---|---|---|
| [17.6]?$\leftarrow X\,^2\Delta_{5/2}$ | 0–0 | 17 643.64[d] | 17 643.59 | 0.05 | | |
| | 1–0 | 17 820.57[d] | 17 823.06 | −2.49 | | |
| | 2–0 | 17 998.76[d] | 17 998.24 | 0.52 | | 41.3 ±5.8 |
| | 3–0 | 18 169.37[d] | 18 169.14 | 0.23 | | 31.1 ±3.9 |
| | 4–0 | 18 336.95[d] | 18 335.76 | 1.19 | | |
| | 5–0 | 18 497.30[d] | 18 498.10 | −0.80 | | |
| | 6–0 | 18 657.17[d] | 18 656.15 | 1.02 | | |
| | 7–0 | 18 810.49[d] | 18 909.93 | 0.56 | | |
| | 8–0 | 18 959.14[d] | 18 959.42 | −0.28 | | |
| | 2–1 | 17 713.82[d] | 17 710.04 | 3.78 | | |
| | 3–1 | 17 881.23[d] | 17 880.94 | 0.29 | | |
| | 4–1 | 18 043.50[d] | 18 047.56 | −4.06 | | |
| [19.6]1.5$\leftarrow X\,^2\Delta_{5/2}$ | 0–0 | 19 612.0295(19)[e] | 19 611.36 | 0.67 | 0.00[f] | 10.7 ±3.1 |
| | 1–0 | 19 789.2425(26)[e] | 19 789.20 | −0.96 | +0.15[f] | 5.99±0.53 |
| | 2–0 | 19 971.37[d] | 19 971.74 | −0.37 | | |
| | 3–0 | 20 156.17[d] | 20 155.97 | 0.20 | | |
| | 4–0 | 20 344.09[d] | 20 342.89 | 1.20 | | |
| | 5–0 | 20 531.76[d] | 20 532.51 | −0.75 | | |

[a]Bands were fit to the standard expression $\nu = T_0 + \omega'_e v' - \omega'_e x'_e(v'^2 + v') - \Delta G''_{1/2} v''$ for $v''=0,1$, yielding the following fitted values ($1\sigma$ error limits in parentheses): [17.6]?$\leftarrow X\,^2\Delta_{5/2}$ system: $T_0$=17 643.59(1.79) $cm^{-1}$, $\omega'_e$ = 183.75(1.17) $cm^{-1}$, $\omega'_e x'_e$ = 2.14(0.13) $cm^{-1}$, $\Delta G''_{1/2}$ = 288.20(1.66) $cm^{-1}$. [19.6]1.5$\leftarrow X\,^2\Delta_{5/2}$ system: $T_0$=19 611.36(99) $cm^{-1}$, $\omega'_e$ = 176.14(1.10) $cm^{-1}$, $\omega'_e x'_e$ = −1.35(0.18) $cm^{-1}$.
[b]Defined as $\nu - \nu_{calc}$.
[c]Defined as $\nu_0(^{194}Pt\ ^{63}Cu) - \nu_0(^{195}Pt\ ^{63}Cu)$.
[d]Measured in low resolution (0.7 $cm^{-1}$).
[e]Measured in high resolution (0.04 $cm^{-1}$) as the band origin, $\nu_0$, calibrated using the $I_2$ atlas. The $1\sigma$ error limit is given in parentheses.
[f]Measured in high resolution (0.04 $cm^{-1}$).

### C. Vibronic spectrum of $^{195}Pt^{63}Cu$

Figure 5 displays a small portion of the low-resolution vibronic spectrum of $^{195}$Pt $^{63}$Cu, which was collected using coumarin 540A, fluorescein 548, and rhodamine 590 dye laser radiation for excitation, with ArF excimer radiation for photoionization. Although platinum possesses four naturally occurring isotopes in greater than 5% natural abundance [$^{194}$Pt (32.9%), $^{195}$Pt (33.8%), $^{196}$Pt (25.3%), and $^{198}$Pt (7.2%)] and copper occurs both as $^{63}$Cu (69.17%) and $^{65}$Cu (30.83%), the mass 258 combination consists purely of $^{63}$Cu $^{195}$Pt and is the most abundant of the copper–platinum isotopomers. For this reason it is chosen as the reference isotopic species for this work.

Numerous presumably isolated vibronic transitions were observed in this molecule, but only two vibrational progressions could be identified. These are listed in Table III along with the results of vibrational fits to extract $\omega_e$ and $\omega_e x_e$. The lifetime of the excited state forming the progression in Fig. 5 has been measured as $\tau = 41 \pm 6\ \mu s$ for $v'=2$ and $31 \pm 4\ \mu s$ for $v'=3$, implying a maximum possible absorption oscillator strength of $1.5 \times 10^{-4}$ for this band system, assuming that the upper state decays purely by fluorescence to the ground electronic state. Since this would be a rather weak absorption system, it would seem that the excellent signal-to-noise ratio displayed in Fig. 5 is due to efficient production of diatomic PtCu. In the case of the vibrational progression shown in Fig. 5, it was possible to identify vibrational hot bands, which allowed the vibrational interval of the ground state to be measured as $\Delta G'_{1/2}$ = 288.2 $cm^{-1}$. Unfortunately, attempts to rotationally resolve the band system displayed in Fig. 5 were not successful.

The second vibrational progression listed in Table III lies to the blue of the optical region shown in Fig. 5. In this case the excited-state lifetime was somewhat reduced, and rotationally resolved spectra were successfully obtained and analyzed. The results of these rotational analyses are given in the next subsection.

### D. Rotationally resolved spectra of $^{195}Pt^{63}Cu$

#### 1. The 0–0 band of the [18.7]2.5$\leftarrow X\,^2\Delta_{5/2}$ band system of PtCu

The relatively intense band located at 18 700 $cm^{-1}$ (between the 6–0 and 7–0 bands of the progression shown in Fig. 5) has been rotationally resolved in Fig. 6. This band does not appear as part of a readily identifiable progression. Although the signal-to-noise ratio of the spectrum displayed in Fig. 6 is not as good as one would like, it is nevertheless clear why this particular electronic state fails to display a vibrational progression in transitions with the ground state: The presence of an undegraded $Q$ branch and $R$ and $P$ branches which fan out symmetrically indicates only a very small change in bond length upon electronic excitation. As a result, the Franck–Condon factors for higher $v'$–0 bands become prohibitively small, and the

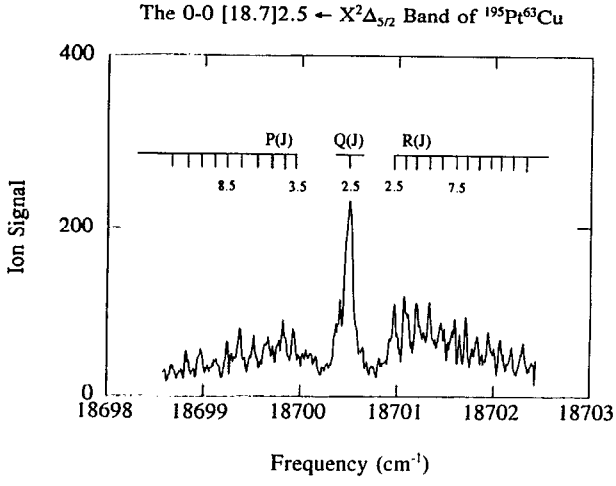


FIG. 6. High-resolution (0.04 $cm^{-1}$) scan over the 0–0 band of the $[18.7]2.5 \leftarrow X\,^2\Delta_{5/2}$ system of $^{195}Pt\,^{63}Cu$. The spectrum fans out nearly symmetrically from the undegraded $Q$ branch, indicating little change in bond length upon electronic excitation.

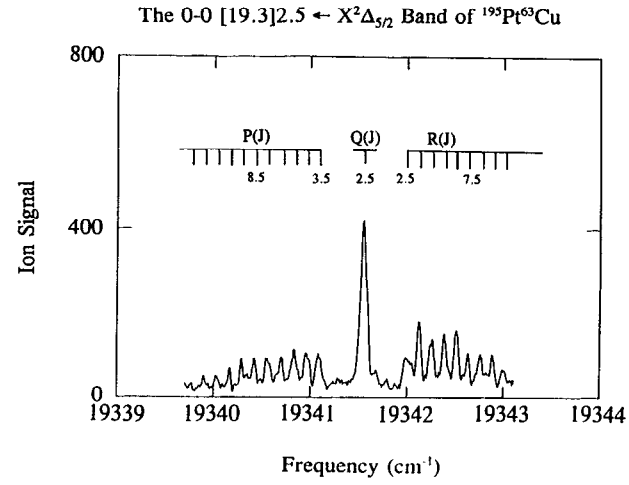


FIG. 7. High-resolution (0.04 $cm^{-1}$) scan over the 0–0 band of the $[19.3]2.5 \leftarrow X\,^2\Delta_{5/2}$ system of $^{195}Pt\,^{63}Cu$. As in Fig. 6, the spectrum fans out nearly symmetrically from an undegraded $Q$ branch, again indicating only a minor change in bond length upon electronic excitation.

higher bands are not observed. A further indication that this is an origin band is provided by the small negative isotope shift measured between the $Q$ branches of the $^{194}Pt\,^{63}Cu$ and $^{195}Pt\,^{63}Cu$ isotopes, given by $\nu_0(^{194}Pt\,^{63}Cu) - \nu_0(^{195}Pt\,^{63}Cu) = -0.013\ cm^{-1}$.

In addition to having a nearly symmetrical rotational structure, the 18 700 $cm^{-1}$ band of PtCu displays nearly equal intensity in the $P$ and $R$ branches, indicating a $\Delta\Omega = 0$ transition. Furthermore, it is immediately evident that a large gap exists between the first $R$ and $Q$ lines, and between the first $Q$ and $P$ lines. This indicates a relatively large value of $\Omega$ in the ground and excited states. Detailed analysis of the spectrum shows $\Omega' = \Omega'' = 5/2$, so in keeping with the notation described for NiAu, the band is assigned as the 0–0 band of the $[18.7]2.5 \leftarrow X\,^2\Delta_{5/2}$ system. Again, the ground state is assumed to derive from the $5d^9 6s^1$, $^3D$ (Pt) $+ 3d^{10}4s^1$, $^2S$ (Cu) separated atom limit, which gives bound electronic states which may be characterized as $5d^9_{Pt}3d^{10}_{Cu}\sigma^2$. The observation of an $\Omega'' = 5/2$ ground state then implies that the $5d$ hole on platinum is in the $5d\delta$ orbital, which is completely analogous to our observations for NiCu (Refs. 7 and 8) and NiAu, and is also in agreement with the predictions of a simple ligand-field calculation.[9]

Measured and fitted line positions for all of the rotationally resolved bands of PtCu are available[25] from the Physics Auxiliary Publication Service (PAPS) of the American Institute of Physics or from one of the authors (M. D. M.). The results of the least-squares fit of the line positions of this and the other rotationally resolved bands of PtCu to Eq. (3.1) are provided in Table IV.

### 2. The 0–0 band of the $[19.3]2.5 \leftarrow X\,^2\Delta_{5/2}$ band system of PtCu

Figure 7 displays a rotationally resolved scan over another isolated band which is not part of an obvious vibrational progression. This is very similar to the band displayed in Fig. 6, in that the band is undegraded, indicating a very minor change in bond length upon electronic excitation. As a result it should again come as no surprise that this system does not form an extended progression. The assignment of this band as an origin band is again confirmed by a small negative isotope shift of $\nu_0(^{194}Pt\,^{63}Cu) - \nu_0(^{195}Pt\,^{63}Cu) = -0.006\ cm^{-1}$. Further, the near equal intensity of the $P$ and $R$ branches again suggests a $\Delta\Omega = 0$ transition, as is confirmed by detailed analysis. The final constants extracted from the fit of this 0–0 band of the $[19.3]2.5 \leftarrow X\,^2\Delta_{5/2}$ system of PtCu are given in Table IV.

TABLE IV. Results from rotationally resolved studies of $^{195}Pt\,^{63}Cu$.[a]

| System | Band | $\nu_0$ ($cm^{-1}$) | $B'_{v'}$ ($cm^{-1}$) | $B''_0$ ($cm^{-1}$) |
|---|---|---|---|---|
| $[18.7]2.5 \leftarrow X\,^2\Delta_{5/2}$ | 0–0[b] | 18 700.5060(31) | 0.064 53(10) | 0.064 96(10) |
| $[19.3]2.5 \leftarrow X\,^2\Delta_{5/2}$ | 0–0[c] | 19 341.5416(25) | 0.064 70(10) | 0.064 89(9) |
| $[19.6]1.5 \leftarrow X\,^2\Delta_{5/2}$ | 0–0[d] | 19 612.0295(19) | 0.061 84(8) | 0.065 22(8) |
| | 1–0[e] | 19 789.2425(26) | 0.061 64(10) | 0.064 70(10) |

[a]All values are reported in wavenumbers ($cm^{-1}$), with $1\sigma$ error limits in parentheses.
[b]Lifetime of the upper state measured as $\tau = 6.50 \pm 1.82\ \mu s$ ($1\sigma$ error limit).
[c]Lifetime of the upper state measured as $\tau = 6.99 \pm 0.32\ \mu s$ ($1\sigma$ error limit).
[d]Lifetime of the upper state measured as $\tau = 10.7 \pm 3.1\ \mu s$ ($1\sigma$ error limit).
[e]Lifetime of the upper state measured as $\tau = 5.99 \pm 0.53\ \mu s$ ($1\sigma$ error limit).

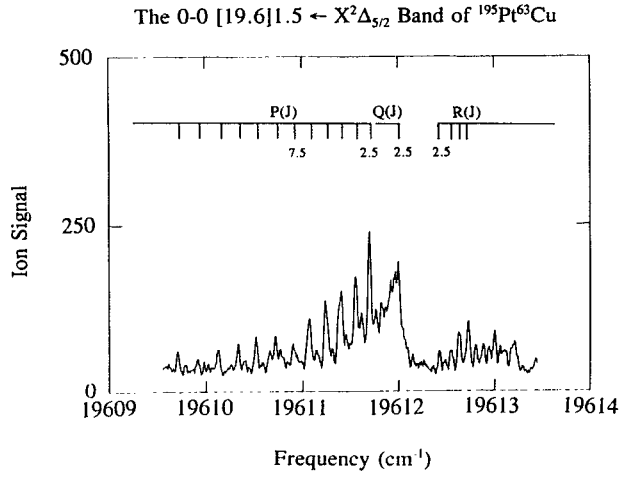


FIG. 8. High-resolution (0.04 $cm^{-1}$) scan over the 0–0 band of the $[19.6]1.5 \leftarrow X\,^2\Delta_{5/2}$ system of $^{195}Pt\,^{63}Cu$. This red-shaded spectrum displays much greater intensity in the $P$ branch than in the $R$ branch, as is indicative of a $\Delta\Omega = -1$ transition. The formation of a head in the $R$ branch indicates significant lengthening of the bond upon electronic excitation.

### 3. The 0–0 and 1–0 Bands of the $[19.6]1.5 \leftarrow X\,^2\Delta_{5/2}$ Band System of PtCu

The 0–0 and 1–0 bands of the second identifiable vibronic progression of PtCu have also been rotationally resolved and analyzed. A rotationally resolved scan over the 0–0 band is displayed in Fig. 8. Unlike the rotationally resolved bands described above, this band is red-shaded and displays $P$ and $Q$ branches which are much more intense than the $R$ branch. This observation indicates a $\Delta\Omega = -1$ transition or an $\Omega' = 3/2 \leftarrow X\,^2\Delta_{5/2}$ transition. Again this is verified by a detailed analysis. The results of a least-squares fit of the observed line positions for the 0–0 and 1–0 bands are again provided in Table IV.

## E. Ionization potentials of NiAu and PtCu

### 1. IP(NiAu)

During the course of these spectroscopic investigations, the ionization potential of NiAu was bracketed. The lowest-frequency transition observed in NiAu using ArF (6.423 eV) radiation for photoionization was the 0–0 band of the $[18.4]2.5 \leftarrow X\,^2\Delta_{5/2}$ system, with its band origin at 18 402.15 $cm^{-1}$ (2.282 eV). This places the ionization potential of NiAu below 8.705 eV. Spectra of NiAu could also be collected using $F_2$ radiation (7.866 and 7.871 eV) for photoionization, thereby bracketing the ionization potential of NiAu in the range $7.866\ eV < IP(NiAu) < 8.705$ eV. In addition, however, a transition in NiAu was observed at 12 340 $cm^{-1}$ (1.530 eV) using $F_2$ radiation for photoionization, but this transition could not be observed using ArF radiation (6.423 eV) for photoionization. This places the ionization potential of NiAu above 7.953 eV. Together these results bracket the ionization potential of NiAu in the range $7.953\ eV < IP(NiAu) < 8.705$ eV, giving $IP(NiAu) = 8.33 \pm 0.38$ eV. This is quite close to the ionization potentials determined for the related $3d$–$5d$ intermetallic diatomics NiPt ($8.02 \pm 0.15$ eV) (Ref. 5) and CuAu ($8.74 \pm 0.05$ eV).[3]

### 2. IP(PtCu)

In the case of PtCu, it has proven possible to obtain an even more restrictive bracketing of the ionization potential. Using ArF radiation (6.423 eV) to provide the second, ionizing photon in the resonant two-photon ionization experiment, transitions were observed as far to the red as 15 408 $cm^{-1}$ (1.910 eV), but no transitions were observed beyond this frequency with ArF radiation. From this observation it may be concluded that the ionization potential of PtCu lies in the range $6.423\ eV < IP(PtCu) < 8.333$ eV. Using $F_2$ radiation (7.866 and 7.871 eV) for photoionization, however, allowed new bands to be observed beginning at 14 293 $cm^{-1}$ (1.772 eV) and extending further to the red. Since this band could not be observed using ArF radiation (6.423 eV), one must conclude that the ionization potential of PtCu lies above 8.195 eV, leading to the improved IP bracket of $8.195\ eV < IP(PtCu) < 8.333$ eV, or $IP(PtCu) = 8.26 \pm 0.07$ eV. Again, this is quite close to the ionization potentials of NiPt ($8.02 \pm 0.15$ eV), NiAu ($8.33 \pm 0.38$ eV), and CuAu ($8.74 \pm 0.05$ eV).

## F. Reinvestigation of mass spectroscopic values of $D_0^0$(NiAu)

In 1968 Kant investigated the equilibrium

$$NiAu + Au \overset{K}{\rightleftharpoons} Au_2 + Ni \tag{3.2}$$

by high-temperature Knudsen effusion mass spectrometry, obtaining values of $D_0^0(NiAu)$ of $2.52 \pm 0.22$ eV (second-law method) or $2.60 \pm 0.22$ eV (third-law method).[22] Although these values agree within the quoted error limits, the fact that the third-law value exceeds that obtained by the second-law method indicates that the partition function of NiAu was underestimated in the third-law calculation. As has been discussed elsewhere,[27] this is a common difficulty, since the number of thermally accessible low-lying electronic states which exist in a diatomic transition metal is notoriously difficult to estimate. Based on our success in using a ligand-field model to predict the location of the low-lying electronic states of NiCu,[9] we have employed this model to predict the location of the analogous states of NiAu. This leads to a prediction of $\Omega = 3/2$ states lying 735.5 and 1978.8 $cm^{-1}$ above the $^2\Delta_{5/2}$ ground state, and $\Omega = 1/2$ states 1542.4 and 3070.1 $cm^{-1}$ above the $^2\Delta_{5/2}$ ground state. These energies were employed in a revised calculation of the third-law bond strength of NiAu, with the additional assumption that $\omega_e = 270$ $cm^{-1}$ and $r_e = 2.351$ Å for all five low-lying states. Finally, the (slightly) revised bond strength $D_0^0(Au_2) = 2.290 \pm 0.008$ eV (Ref. 4) was employed in the calculation, to give a revised third-law value of $D_0^0(NiAu) = 2.52 \pm 0.16$ eV. The slight revision of the bond strength of $Au_2$ also modified the second-law value (mainly by reducing the error limit) to give $D_0^0(NiAu) = 2.52 \pm 0.17$ eV.

TABLE V. Electronic states of $^{58}Ni\ ^{197}Au$.[a]

| State | $T_0$ (cm$^{-1}$) | $\omega_e$ (cm$^{-1}$) | $\omega_e x_e$ (cm$^{-1}$) | $B_e$ (cm$^{-1}$) | $\alpha_e$ (cm$^{-1}$) | $r_e$ (Å) | Lifetime ($\mu$s) |
|---|---|---|---|---|---|---|---|
| [18.5]1.5 | 18 510.9976(18) | | | $B_0$=0.063 90(7) | | $r_0$=2.428(1) | 14.7(5) |
| [18.4]2.5 | 18 402.1483(24) | 79.45(1.03) | 0.00(0.11) | 0.059 37(10) | 0.000 93(7) | 2.519(2) | 6.8(1) |
| $X\ ^2\Delta_{5/2}$ | 0.00 | | | $B_0$=0.068 12(5) | | $r_0$=2.351(1) | |

[a] $IP$(NiAu)=8.33±0.38 eV; $D_0$(NiAu)=2.52±0.17 eV; $D_0$(Ni$^+$–Au)=1.81±0.42 eV; $D_0$(Ni–Au$^+$)=3.41±0.42 eV. Uncertainties are given in parentheses in the table, as 1$\sigma$ error limits.

## IV. DISCUSSION

A summary of what is currently known about the ground and excited electronic states of NiAu is provided in Table V, and the corresponding information about PtCu is given in Table VI. The single most important determination provided by the present investigation is that diatomic NiAu and PtCu have the same ground electronic state symmetry, $X\ ^2\Delta_{5/2}$, as their congener, NiCu.[7,8] In these molecules the ground $X\ ^2\Delta_{5/2}$ state derives from the combination of a $d^9s^1(^3D)$ nickel or platinum atom with a $d^{10}s^1(^2S)$ coinage group atom. The $d^{10}s^1(^2S_{1/2})$ state for the coinage group atoms is the ground state, while the $d^9s^1(^3D_3)$ level is the ground level for platinum and lies only 204.786 cm$^{-1}$ above the ground level for nickel.[28] As a result there is little or no promotion energy required to prepare the atoms for bonding in this series of molecules, which all possess a ground configuration of $d_A^9d_B^{10}\sigma^2$.

It is interesting that in all three cases, NiCu, NiAu, and PtCu, the ground level is the $^2\Delta_{5/2}$ state deriving from this $d_A^9d_B^{10}\sigma^2$ configuration. This result runs counter to what would be expected if there were significant $d$-orbital overlap between the two metal centers, since then the $d$ orbitals would combine to form bonding and antibonding orbitals, with the orbitals falling in the energetic order $d\sigma < d\pi < d\delta < d\delta^* < d\pi^* < d\sigma^*$. If the $d$ orbitals were strongly split into bonding and antibonding orbitals in this way, the single $d$ hole in the $d_A^9d_B^{10}\sigma^2$ configuration would undoubtedly reside in the $d\sigma^*$ orbital, leading to a $^2\Sigma^+$ ground state. The fact that this is not observed is a strong indication that the $d$ orbitals are *not* strongly split into bonding and antibonding orbitals.

The observation of a $^2\Delta_{5/2}$ ground state for all three molecules is consistent with the predictions of a simple ligand-field theory which incorporates spin–orbit coupling, however.[9] In this model the $d_A^9d_B^{10}\sigma^2$ manifold of states is considered as a combination of a $d_A^9$ and a $d_B^{10}$ ion separated by the equilibrium bond length and neutralized by a relatively diffuse $\sigma^2$ cloud of electrons. The $d_A^9$, $^2D$ ion is then split into its component states by interaction with the +1 ion core of the $d_B^{10}$ ion, which has been approximated as a point charge.[9] Finally, the spin–orbit coupling of the orbital and spin angular momenta of the $d$ hole must also be included. The electrostatic potential of the positive charge of the $d_B^{10}$ ion has the effect of stabilizing the $d\sigma$ orbital of the $d_A^9$ ion, since this orbital is directed toward the positive charge. The $d\pi$ orbital is also stabilized by this effect but to a lesser extent, and the $d\delta$ orbital lies highest in energy. Thus, the electrostatic effect favors the placement of the hole in the highest-energy orbital, which is $d\delta$ in symmetry. The emergence of the $^2\Delta_{5/2}$ state as the ground state is therefore a strong indication that the $d$ orbitals are substantially nonbonding in the NiCu, NiAu, and PtCu diatomic molecules.

Of course, it is impossible for the $3d$–$5d$ mixed transition-metal molecule CuAu to possess significant $d$-orbital contributions to the bond in its ground electronic state, since this state is a $^1\Sigma^+$ state deriving from the $3d_{Cu}^{10}5d_{Au}^{10}\sigma^2$ configuration. The presence of filled $d$ subshells in the ground state of CuAu guarantees that no significant $d$-orbital bonding can be present. In this regard it is of interest to compare the bond lengths of NiAu and PtCu to their filled $d$-orbital counterpart (CuAu), to verify that NiAu and PtCu lack significant $d$-orbital contributions to the bonding, as is implied by their $^2\Delta_{5/2}$ ground states. This comparison is provided in Table VII, where it is clear that the bond lengths of CuAu, PtCu, and NiAu are very similar (2.34±0.01 Å), but NiPt displays a much shorter bond length (2.208 Å). On the basis of these bond lengths, it would appear that there are no significant $d$-orbital contributions to the bonding in NiAu or PtCu, but a substantial bonding contribution is present in NiPt. Evidence of this is also available from the measured bond strengths of these species, with NiPt having a significantly greater bond strength than either NiAu or CuAu.

Table VII presents all of the presently known data for the nickel and copper group diatomic molecules in their

TABLE VI. Electronic states of $^{195}Pt\ ^{63}Cu$.[a]

| State | $T_0$ (cm$^{-1}$) | $\omega_e$ (cm$^{-1}$) | $\omega_e x_e$ (cm$^{-1}$) | $B_e$ (cm$^{-1}$) | $\alpha_e$ (cm$^{-1}$) | $r_e$ (Å) | Lifetime ($\mu$s) |
|---|---|---|---|---|---|---|---|
| [19.6]1.5 | 19 612.0295(19) | 176.14(1.10) | −1.35(0.18) | 0.061 94(12) | 0.000 20 | 2.392(2) | 6.1(0.5) |
| [19.3]2.5 | 19 341.5416(25) | | | $B_0$=0.064 70(10) | | $r_0$=2.340(2) | 7.0(0.3) |
| [18.7]2.5 | 18 700.5060(31) | | | $B_0$=0.064 53(10) | | $r_0$=2.343(2) | 6.5(1.8) |
| [17.6]? | 17 643.64 | 183.75(1.17) | 2.14(0.13) | | | | 34.3(3.2) |
| $X\ ^2\Delta_{5/2}$ | 0.00 | $\Delta G''_{1/2}$=288.20(1.66) | | $B_0$=0.064 97(5) | | $r_0$=2.3353(8) | |

[a] IP(PtCu)=8.26±0.07 eV. Uncertainties are given in parentheses in the table, as 1$\sigma$ error limits.

TABLE VII. Comparison of the nickel and copper group diatomic molecules.

| | 20 electrons | 21 electrons | | 22 electrons |
|---|---|---|---|---|
| 3*d*–3*d* | $Ni_2$<br>$\Omega=4(?)$[b,c]<br>$r_0=2.20(1)$ Å[b,c]<br><br>$D_0^0=2.068$ eV[b]<br>$IP=7.63(7)$ eV[f] | NiCu[a]<br>$^2\Delta_{5/2}$<br>$r_0=2.2346(5)$ Å<br>$\omega_e=273.01(1.15)$ cm$^{-1}$<br>$D_0^0=2.05(10)$ eV | | $Cu_2$<br>$^1\Sigma_g^+$<br>$r_e=2.2197$ Å[d]<br>$\omega_e=266.43$ cm$^{-1}$ [e]<br>$D_0^0=2.03(2)$ eV [c]<br>$IP=7.899(7)$ eV [g] |
| 3*d*–4*d* | NiPd[c,h]<br>$\Omega=2$<br>$r_0=2.242(5)$ Å<br><br>$D_0^0\approx 1.43$ eV<br>$IP=7.18(76)$ eV | NiAg | CuPd | CuAg<br>$^1\Sigma^+$<br>$r_0=2.3735(6)$ Å[i]<br>$\Delta G_{1/2}=229.2(3)$ cm$^{-1}$ [i]<br>$D_0^0=1.74(10)$ eV [c]<br>$IP=7.7806(4)$ eV [j] |
| 4*d*–4*d* | $Pd_2$<br>$(^3\Sigma_u^+)$[k]<br><br>$\omega_e=210(10)$ cm$^{-1}$ [m]<br>$D_0^0=1.03(16)$ eV [n] | PdAg | | $Ag_2$<br>$^1\Sigma_g^+$<br>$r_e=2.531$ Å[l]<br>$\omega_e=192.4$ cm$^{-1}$ [d]<br>$D_0^0=1.67(4)$ eV [o]<br>$IP=7.56(2)$ eV [o] |
| 3*d*–5*d* | NiPt[p]<br>$\Omega=0$<br>$r_0=2.208(2)$ Å<br><br>$D_0^0=2.798(3)$ eV<br>$IP=8.02(15)$ eV | NiAu[q]<br>$^2\Delta_{5/2}$<br>$r_0=2.351(1)$ Å<br><br>$D_0^0=2.52(17)$ eV<br>$IP=8.33(38)$ eV | PtCu[q]<br>$^2\Delta_{5/2}$<br>$r_0=2.3353(8)$ Å<br>$\Delta G_{1/2}=288(2)$ cm$^{-1}$<br><br>$IP=8.26(7)$ eV | CuAu[r]<br>$^1\Sigma^+$<br>$r_0=2.3302(6)$ Å<br>$\Delta G_{1/2}=248.35$ cm$^{-1}$<br>$D_0^0=2.344(19)$ eV<br>$IP=8.74(5)$ eV |
| 4*d*–5*d* | PdPt[c,h]<br><br>$D_0^0\approx 1.98$ eV<br>$IP=8.27(38)$ eV | PdAu | PtAg | AgAu<br>$^1\Sigma^+$<br>$D_0^0=2.06(10)$ eV [s] |
| 5*d*–5*d* | $Pt_2$ [t]<br><br><br><br>$D_0^0=3.14(2)$ eV<br>$IP=8.68(2)$ eV | PtAu | | $Au_2$<br>$^1\Sigma_g^+$<br>$r_e=2.4715$ Å[u]<br>$\omega_e=190.9$ cm$^{-1}$ [d]<br>$D_0^0=2.290(8)$ eV [v]<br>$IP=9.20(21)$ eV [v] |

[a]References 7 and 8.
[b]Reference 11.
[c]Reference 13.
[d]Reference 15.
[e]Reference 30.
[f]Reference 29.
[g]Reference 31.
[h]Reference 6.
[i]Reference 1.
[j]Reference 32.
[k]Reference 33.
[l]Reference 36.
[m]Reference 34.
[n]Reference 35.
[o]Reference 27.
[p]Reference 5.
[q]This work.
[r]Reference 2.
[s]Reference 37.
[t]Reference 12.
[u]Reference 16.
[v]Reference 4.

ground electronic states. It is clear from a brief glance that the chemical bonding in $Ni_2$, NiCu, and $Cu_2$ is essentially identical, since all three species have nearly the same bond lengths and bond strengths. On the other hand, the much greater bond strength of $Pt_2$ as compared to $Au_2$ argues for strong participation of the 5*d* orbitals in the chemical bonding in the $d_A^9 d_B^9 \sigma^2$ molecule, $Pt_2$. This is undoubtedly the result of a relativistic expansion of the 5*d* orbitals, which makes them much more accessible for chemical bonding.[27] In this regard it will be very interesting to obtain a measurement of the bond length of $Pt_2$ and to investigate the bond length and bond strength of PtAu. Finally, the significantly shorter bond length of NiPd as compared to CuAg suggests a definite 3*d*–4*d* bonding interaction in NiPd, although this may not be manifested in the bond strength because of the inherent stability of the $4d^{10}5s^0$ configuration of Pd.

## V. CONCLUSION

In the present work, both vibrationally and rotationally resolved resonant two-photon ionization spectra have been obtained for NiAu and PtCu. The ground electronic states have been determined to be $^2\Delta_{5/2}$ for both species, and are thought to derive from $d_A^9 d_B^{10} \sigma^2$ molecular configurations. The emergence of $^2\Delta_{5/2}$ as the ground state is consistent with the absence of significant *d*-orbital contributions to the bonding in either species. This conclusion is also supported by the measured bond lengths ($r_0$) of 2.351 $\pm$0.001 and 2.335$\pm$0.001 Å, for NiAu and PtCu, respec-

tively, which are nearly identical to that measured for CuAu ($r_0 = 2.330 \pm 0.001$ Å).[3] The determination of $^2\Delta_{5/2}$ as the ground state of NiAu and PtCu is consistent with that of the congener, NiCu, and is also consistent with a ligand-field model of the molecules, in which the Ni or Pt $d^9$ core is electrostatically perturbed by the localized $+1$ charge of the core of the other atom.[9] It remains to be seen to what extent this model will succeed in predicting the energetics of the remaining states of the $d_A^9 d_B^{10}\sigma^2$ molecular configuration in these molecules.

In addition to these results, the ionization potentials have been bracketed as IP(NiAu) $= 8.33 \pm 0.38$ eV and IP(PtCu) $= 8.26 \pm 0.07$ eV, and the vibrational interval of ground state $^{195}$Pt $^{63}$Cu has been measured as $288.2 \pm 1.7$ cm$^{-1}$. Finally, a reanalysis of previous measurements by high-temperature Knudsen effusion mass spectrometry has provided $D_0^0$(NiAu) $= 2.52 \pm 0.17$ eV.

## ACKNOWLEDGMENTS

We thank Professor William H. Breckenridge for the use of the intracavity étalon used in the high-resolution studies. We gratefully acknowledge research support from the National Science Foundation under Grant No. CHE-8912673. Acknowledgment is also made to the donors of the Petroleum Research Fund, administered by the American Chemical Society, for partial support of this research.

[1] G. A. Bishea, N. Marak, and M. D. Morse, J. Chem. Phys. **95**, 5618 (1991).
[2] G. A. Bishea and M. D. Morse, Chem. Phys. Lett. **171**, 430 (1990).
[3] G. A. Bishea, J. C. Pinegar, and M. D. Morse, J. Chem. Phys. **95**, 5630 (1991).
[4] G. A. Bishea and M. D. Morse, J. Chem. Phys. **95**, 5646 (1991).
[5] S. Taylor, E. M. Spain, and M. D. Morse, J. Chem. Phys. **92**, 2698 (1990).
[6] S. Taylor, E. M. Spain, and M. D. Morse, J. Chem. Phys. **92**, 2710 (1990).
[7] Z.-W. Fu and M. D. Morse, J. Chem. Phys. **90**, 3417 (1989).
[8] E. M. Spain and M. D. Morse, J. Chem. Phys. **97**, 4633 (1992).
[9] E. M. Spain and M. D. Morse, J. Chem. Phys. **97**, 4641 (1992).
[10] J. G. McCaffrey, R. R. Bennett, M. D. Morse, and W. H. Breckenridge, J. Chem. Phys. **90**, 92 (1989).
[11] M. D. Morse, G. P. Hansen, P. R. R. Langridge-Smith, Lan-Sun Zheng, M. E. Geusic, D. L. Michalopoulos, and R. E. Smalley, J. Chem. Phys. **80**, 5400 (1984).
[12] S. Taylor, G. W. Lemire, Y. Hamrick, Z.-W. Fu, and M. D. Morse, J. Chem. Phys. **89**, 5517 (1988).
[13] M. D. Morse, *Advances in Metal and Semiconductor Clusters, Vol. I. Spectroscopy and Dynamics* (JAI, Greenwich, in press).
[14] I. Shim, Theor. Chim. Acta. **54**, 113 (1980).
[15] K. P. Huber and G. Herzberg, *Molecular Spectra and Molecular Structure. IV. Constants of Diatomic Molecules* (Van Nostrand Reinhold, New York, 1979).
[16] L. L. Ames and R. F. Barrow, Trans. Faraday Soc. **63**, 39 (1967).
[17] J. P. Desclaux, At. Data Nucl. Data **12**, 311 (1973).
[18] Z.-W. Fu, G. W. Lemire, Y. Hamrick, S. Taylor, J.-C. Shui, and M. D. Morse, J. Chem. Phys. **88**, 3524 (1988).
[19] E. M. Spain, J. M. Behm, and M. D. Morse, Chem. Phys. Lett. **179**, 411 (1991).
[20] E. M. Spain and M. D. Morse, J. Phys. Chem. **96**, 2479 (1992).
[21] K. Hilpert and K. A. Gingerich, Ber. Bunsenges. Phys. Chem. **84**, 739 (1980).
[22] A. Kant, J. Chem. Phys. **49**, 5144 (1968).
[23] S. Gerstenkorn and P. Luc, *Atlas du Spectre d'Absorption de la Molecule d'Iode* (CNRS, Paris, 1978); S. Gerstenkorn and P. Luc, Rev. Phys. Appl. **14**, 791 (1979).
[24] G. Herzberg, *Molecular Spectra and Molecular Structure. I. Spectra of Diatomic Molecules*, 2nd ed. (Van Nostrand Reinhold, New York, 1950), p. 208.
[25] See AIP document No. PAPS JCPSA-97-4605-6 for 6 pages of tables giving measured and fitted rotational line positions for $^{58}$Ni $^{197}$Au and $^{195}$Pt $^{63}$Cu. Order by PAPS number and journal reference from American Institute of Physics, Physics Auxiliary Publication Service, 335 East 45th Street, New York, NY 10017. The price is $1.50 for each microfiche (60 pages) or $5.00 for photocopies of up to 30 pages, and $0.15 for each additional page over 30 pages. Airmail additional. Make checks payable to the American Institute of Physics.
[26] C. Linton, M. Dulick, R. W. Field, P. Carete, P. C. Leyland, and R. F. Barrow, J. Mol. Spectrosc. **102**, 441 (1983).
[27] M. D. Morse, Chem. Rev. **86**, 1049 (1986).
[28] C. E. Moore, Natl. Bur. Stand. (U.S.) Circ. 467 (1971).
[29] Li Lian, Ph.D. thesis, University of Utah, 1992 (unpublished).
[30] E. A. Rohlfing and J. J. Valentini, J. Chem. Phys. **84**, 6560 (1986).
[31] A. D. Sappey, J. E. Harrington, and J. C. Weisshaar, J. Chem. Phys. **91**, 3854 (1989).
[32] A. M. James, G. W. Lemire, and P. R. R. Langridge-Smith (unpublished).
[33] K. Balasubramanian, J. Chem. Phys. **89**, 6310 (1988).
[34] J. Ho, K. M. Ervin, M. L. Polak, M. K. Gilles, and W. C. Lineberger, J. Chem. Phys. **95**, 4845 (1991).
[35] I. Shim and K. A. Gingerich, J. Chem. Phys. **80**, 5107 (1984).
[36] B. Simard, P. A. Hackett, A. M. James, and P. R. R. Langridge-Smith, Chem. Phys. Lett. **186**, 415 (1991).
[37] M. Ackerman, F. E. Stafford, and J. Drowart, J. Chem. Phys. **33**, 1784 (1960).